Title:

D-serine suppresses one-carbon metabolism by competing with mitochondrial L-serine transport

Masataka Suzuki[1,2,15#], Kenichiro Adachi[1#], Pattama Wiriyasermukul[3, 4], Mariko Fukumura[5], Ryota Tamura[5], Yoshinori Hirano[6, 7], Yumi Aizawa[8, 9], Tetsuya Miyamoto[10], Sakiko Taniguchi[1], Masahiro Toda[5], Hiroshi Homma[10], Kohsuke Kanekura[11], Kenji Yasuoka[6], Takanori Kanai[12], Masahiro Sugimoto[8, 9], Shushi Nagamori[3], Masato Yasui[1], and Jumpei Sasabe[13, 14, 15]

1. Department of Pharmacology, Keio University School of Medicine, 35 Shinanomachi, Shinjuku-ku, Tokyo 160-8582, Japan.
2. Current address; Division of Infectious Diseases, Brigham and Women's Hospital, Boston, MA, USA.
3. Center for SI Medical Research and Department of Laboratory Medicine, The Jikei University School of Medicine, Tokyo, 105-8461, Japan.
4. Current address; Department of Biological Chemistry, Faculty of Agriculture, Iwate University, Iwate, 020-8550, Japan
5. Department of Neurosurgery, Keio University School of Medicine, 35 Shinanomachi, Shinjuku-ku, Tokyo 160-8582, Japan.
6. Department of Mechanical Engineering, Keio University, 3-14-1 Hiyoshi, Kohoku-ku, Yokohama, Kanagawa 223-8522, Japan
7. Laboratory for Computational Molecular Design, RIKEN Center for Biosystems Dynamics Research (BDR), Suita, Osaka 565-0874, Japan
8. Institute of Medical Science, Tokyo Medical University, Shinjuku, Tokyo, Japan
9. Institute for Advanced Biosciences, Keio University, Tsuruoka, Yamagata, Japan
10. Graduate School of Pharmaceutical Sciences, Kitasato University, 5-9-1 Shirokane, Minato-ku, Tokyo 108–8641, Japan
11. Department of Pharmacology, Tokyo Medical University, 6-1-1 Shinjuku, Shinjuku-ku, Tokyo 160-8402, Japan.
12. Department of Internal Medicine, Keio University School of Medicine, 35 Shinanomachi, Shinjuku-ku, Tokyo 160-8582, Japan.
13. Laboratory of Electron Microscope and Chiral Biology, Keio University School of Medicine, 35 Shinanomachi, Shinjuku-ku, Tokyo 160-8582, Japan.
14. Human Biology-Microbiome-Quantum Research Center (WPI-Bio2Q), Keio University, Tokyo 160-8582, Japan
# These authors contributed equally.

15 To whom correspondence should be addressed: Masataka Suzuki and Jumpei Sasabe
Keio University School of Medicine, 35 Shinanomachi, Shinjuku-ku, Tokyo 160-8582 Japan. Phone: +813-5363-3772. E-mail: masataka.s@keio.jp; sasabe@keio.jp

Abstract

L-serine serves as a central metabolic node that integrates glycolytic flux, lipid metabolism, and one-carbon metabolism. In the mature central nervous system, L-serine is actively stereo-converted to D-serine, which functions as a neurotransmitter. However, the role of D-serine in cellular metabolism remains unclear. Here, we show that D-serine competes with mitochondrial L-serine transport, thereby suppressing one-carbon metabolism. Metabolomic analysis revealed that D-serine reduces intracellular glycine and formate levels, indicating inhibition of the initial step of the one-carbon pathway. Molecular dynamics simulations and enzymatic assays revealed that D-serine has low affinity for serine hydroxymethyltransferase 2 (Shmt2), which catalyzes the first step in mitochondrial one-carbon metabolism, and does not directly inhibit its activity. Instead, membrane transport assays demonstrated that D-serine competes with mitochondrial L-serine transport, depleting the substrate of Shmt2. Functionally, under L-serine poor conditions in vitro and ex vivo, D-serine inhibited the proliferation of immature and undifferentiated neural cells including glioblastoma stem cells, which depend highly on one-carbon metabolism. Notably, endogenous D-serine levels were low during early neurodevelopment, but increased with maturation, coinciding with a shift in the transcriptional profiles of serine metabolic enzymes at the cellular level. Given that L-serine supports neurodevelopment and D-serine modulates neurotransmission, this developmental shift in serine enantiomer metabolism appears to align with the functional transitions of the maturing nervous system. Thus, our findings reveal that serine chirality can influence mitochondrial substrate availability and one-carbon flux, offering previously unappreciated insight into the stereoselective regulation of cellular metabolism.

Introduction

Serine is a unique amino acid, both L- and D-enantiomers of which are synthesized *de novo* in the central nervous system. L-serine is primarily synthesized from a glycolytic intermediate through the phosphorylated pathway, and further stereo-converted to D-serine (Fig. 1a). Serine enantiomers and their metabolites are critically involved in neural development and neurophysiology in three major ways. First, L-serine is a crucial carbon donor with the cofactor, folate for the one-carbon metabolism, which is a universal metabolic process for nucleic acid synthesis, methylation, and reductive metabolism. As these pathways essentially support proliferative cells, undifferentiated or cancer cells are particularly susceptible to deprivation of L-serine or inhibition of *de novo* L-serine synthesis(Geeraerts et al., 2021). Second, biosynthesis of membrane lipids requires L-serine as an integral component of sphingolipids and phosphatidylserine. The nervous system includes highly polarized neurons and glia, and has the highest lipid content/complexity in the mammalian body. Among membrane lipids, sphingolipids are particularly abundant in the nervous system and are essential for neuronal differentiation, polarization, synapse formation, and myelination, which are required for development and functional integrity of the nervous system(Hirabayashi and Furuya, 2008). Third, L-serine serves as a precursor for neurotransmitters, such as glycine and D-serine. L-serine is converted to glycine by serine hydroxymethyltransferase (Shmt) in the one-carbon metabolic pathway, and also into D-serine by serine racemase (Srr). Both glycine and D-serine bind physiologically, albeit with different affinities, to the obligatory (GluN1) and regulatory (GluN3) subunits of *N*-methyl-D-aspartate (NMDA) receptors, which regulate excitatory neurotransmission and are crucial in development and functions of the central nervous system(Chatterton et al., 2002; Nancy and Dingledine, 1988). In addition, glycine also binds to inhibitory glycine receptors and controls early embryonic development as well as a variety of motor and sensory functions(Lynch, 2004).

Defects of L-serine synthesis due to single nucleotide polymorphisms in the genes encoding 3-phosphoglycerate dehydrogenase (PHGDH), the rate-limiting enzyme in the phosphorylated pathway, or the downstream enzyme phosphoserine aminotransferase (PSAT1) are associated with congenital microcephaly and hypomyelination, and exhibit psychomotor retardation and seizures in humans (Jaeken et al., 1997; KONING et al., 2002). Phgdh deficient mice die in embryo after 13.5 days post-coitum and show systemic growth defects, especially severe hypoplasia of the central nervous system, with marked reductions of L-serine and sphingolipids(Yoshida et al., 2004). Indeed, proliferative-marker-positive cells and mature neurons are almost entirely absent in these mice, indicating that *de novo* biosynthesis of L-serine is critical for neuronal proliferation and differentiation. Given that L-serine synthesis impacts diverse metabolites in one-carbon metabolism, lipid synthesis, and neurotransmitters glycine and D-serine(Yang et al., 2010), L-serine likely serves multiple functions in neural development. Of note, serine synthesis shows drastic changes after neurogenesis. Neural progenitor cells (NPCs) express PHGDH, whereas mature neurons lack its expression and lose the ability to synthesize L-serine. In mature neural tissue, on the other hand, astrocytes take over L-serine synthesis, and supply neurons with L-serine for synthesis of neurotransmitter D-serine(Wolosker, 2011). This metabolic compartmentalization suggests that D- and L-serine serve distinct functions tailored to the metabolic demands of specific neural cell types and developmental stages. However, how D-serine contributes to cellular metabolism beyond neurotransmission remains largely unknown.

In this study, we employed a metabolomics-based approach to examine how D-serine affects cellular metabolism, identified its primary target pathway in vitro, and assessed the functional consequences in neural cells both in vitro and ex vivo systems.

Main

D-serine impacts metabolites in one-carbon metabolism

To test whether serine chirality influences cellular metabolism in neural tissue, we compared metabolomic profiles of primary cultured neurons (PCNs) treated with or without L- or D-serine. Serine enantiomers markedly altered the levels of metabolites such as glycine, cysteine, hypotaurine, taurine, glutathione, AMP, uracil, and polyamines (Fig. 1A and Fig. S1A and B). These metabolites are components of the one-carbon metabolic network, including the folate cycle and synthetic pathways for purine, glutathione, taurine, and polyamine (Fig. 1B), all of which are initiated by one-carbon donation from L-serine. Compared to D-serine, L-serine affected a broader range of metabolic pathways, including several amino acid metabolism (Fig. 1C and Fig. S1C). Notably, however, D-serine uniquely caused a marked reduction in glycine levels (Fig. 1A), which was further confirmed using a two-dimensional HPLC system (2D HPLC), a highly sensitive tool to quantify enantiomers, to occur independently of any change in L-serine levels (Fig. 1E and F). Metabolites that showed similar reduction patterns to glycine were primarily polyamines and their intermediates (Fig. 1D). Given that glycine is synthesized in the initial step of the one-carbon pathway, and that polyamines are produced in a downstream branch of the one-carbon network (Fig. 1B), these results suggest that D-serine broadly suppresses one-carbon metabolism. In support of our view, D-serine treatment on PCNs further reduced production of formate, an intermediate of the folate cycle in one-carbon metabolism, whereas L-serine enhanced it (Fig. 1G). Therefore, these findings indicate that D-serine exerts an inhibitory effect on the one-carbon metabolism, in contrast to the supportive role of L-serine.

D-serine suppresses one-carbon flux by competing with L-serine transport to mitochondria

In the central nervous system, glycine is synthesized from L-serine by serine hydroxymethyltransferase (Shmt) 1 and 2 (Fig. 2A), which performs the first transfer of a carbon unit from L-serine to folate in one-carbon metabolism (Pan et al., 2020). In the presence of mitochondrial Shmt2, transfer of a carbon unit from L-serine to tetrahydrofolate (THF) and glycine production depends primarily on mitochondrial enzyme, but not cytoplasmic Shmt1 (Fig. 2A)(Ducker et al., 2016). Therefore, the molecular target of D-serine in its inhibition of the initial step of one-carbon metabolism is likely mitochondrial Shmt2 or supply of its substrates into mitochondria (Fig. 2A). To study whether D-serine impacts catalytic activity of Shmt2, we compared homotetrameric assembly of human SHMT2 combined with either L- or D-serine in the presence of THF and pyridoxal phosphate (PLP) (Fig. S2). When L- or D-serine was placed in the binding pocket of Shmt2, the eliminating carbon in D-serine was more distant from phosphorus (P) and oxygen (O) in PLP by 1.50 Å (C-P) and 1.10 Å (C-O) than that in L-serine (Fig. 2B and Fig. S2A and B), suggesting that D-serine is not a good substrate for SHMT2. To investigate the stability of serine enantiomers in the binding pocket, we further performed molecular dynamic (MD) simulation of the serine-bound SHMT2 complex systems. MD simulation indicated that binding of D-serine did not affect the overall structure of SHMT2 compared to that of L-serine (Fig. S2C). On the other hand, molecular interactions of D-serine with SHMT2 were unstable and D-serine could not stay in the serine-binding pocket of SHMT2 (Fig. 2C and Supplementary video 1), which is supported by a recent report that SHMT does not use D-serine as a substrate in the canonical hydroxymethyl-transferase reaction in one-carbon metabolism(Miyamoto et al., 2024). In contrast, L-serine remained placed stably in the pocket (Fig. 2C and Supplementary video 2). Therefore, D-serine was unlikely to compete with L-serine binding to SHMT2. Indeed, an *in vitro* experiment using recombinant SHMT2 showed that D-serine did not affect conversion of L-serine to glycine (Fig. 2D).

Next, we wondered whether D-serine inhibits supply of Shmt2 substrate(s), L-serine or THF, to mitochondria. Since reduction of glycine caused by D-serine in PCNs was compensated by addition of L-serine, but not of THF (Fig. 1E, 2E), we assumed that L-serine supply to mitochondria is disturbed by D-serine. Moreover, in PCNs, endogenous L-serine synthesis was not disturbed by addition of D-serine (Fig. 1F), suggesting that D-serine affects L-serine transport to mitochondria, but not its synthesis. To confirm that D-serine impacts L-serine transport to mitochondria, we semi-permeabilized a neuroblastoma cell line, Neuro2a, to loosen cell membranes and monitored [H^3]L-serine transport into mitochondria and other

organelles in the presence or absence of D-serine. Intriguingly, D-serine competitively inhibited transport of L-serine in a dose-dependent manner (IC50, 1.604 mM) (Fig. 2F). Thus, these results suggested that D-serine impairs one-carbon metabolism by competing with L-serine transport to mitochondria, but not by direct inhibition of Shmt2 activity.

To further understand the overall cellular responses to the D-serine burden, we performed RNA-sequencing using Neuro2a cells treated with D-serine. D-serine mildly, but significantly altered the transcriptome profile compared with vehicle control (Fig. 2G and H). There were 685 up-regulated genes (log_2 fold-change > 0, adjusted p-value < 0.05) and 905 down-regulated genes (log_2-fold change < 0, adjusted p-value < 0.05) (Fig. 2H). To determine whether genes with significant alterations are clustered in specific functional gene sets, we performed gene set enrichment analysis. Notably, D-serine enhanced expressions of genes associated with mitochondrial functions, such as respiratory chain complex assembly, ATP synthesis driven by proton motive force, and mitochondrial gene expression / translation. On the other hand, gene sets linked to amino acid import across the plasma membrane, cellular growth, and neuron projection extension were down-regulated (Fig.2I and J and Fig.S3). These dynamic transcriptional changes in the neuroblastoma cell line indicate that D-serine can impact polarization and growth of immature neurons negatively and further indicate that immature neurons resist D-serine-induced cellular stress by enhancing mitochondrial function, including energy synthesis.

D-serine inhibits proliferation of tumor cells

One-carbon metabolism provides essential metabolites for nucleotide synthesis, methylation, and reductive metabolism, and supports cellular proliferation. Tumor cells are highly proliferative and are particularly susceptible to deprivation of one-carbon units by L-serine restriction or inhibition of *de novo* serine synthesis (Newman and Maddocks, 2017). Given that D-serine inhibits one-carbon flux by competing with L-serine in PCNs and the neuroblastoma cell line, we wondered whether D-serine influences proliferation of neural tumor cells. To test this idea, we treated several human/rodent neuroblastoma cell lines cultured in the regular medium containing sub-millimolar L-serine and fetal bovine serum with D-serine. Consistent with our findings that D-serine competes with L-serine transport (Fig. 2F), high concentrations of D-serine were required to suppress proliferation of neuroblastoma cell lines cultured in regular medium (Fig. S4A). In contrast, culturing in L-serine/glycine-free medium with dialyzed fetal bovine serum reduced the proliferation of Neuro2a cells with much lower D-serine concentrations (IC50 = 1.94 mM) (Fig. S4B-D), which corresponds to the efficacy of D-serine on inhibition of L-serine transport (IC50 = 1.604 mM) (Fig. 2F). Indeed, with L-serine/glycine-free medium, D-serine significantly inhibited proliferation of all neuroblastoma cell lines tested, at low millimolar concentrations (Fig. 3A). In accordance with its effect on PCNs (Fig. 1E), D-serine inhibited production of glycine and suppressed proliferation of Neuro2a cells, which was rescued by supplementation with L-serine (Fig. 3B and Fig. S4E). Moreover, supplementations with glycine and downstream metabolites of the folate cycle in the one-carbon pathway (Fig. 1B), such as formate, inosine monophosphate (IMP), or 5,10-meTHF, phenocopied the rescue effect by L-serine (Fig. S4E-I). On the other hand, combinations of glycine and metabolites of the methionine cycle (methionine or methylcobalamin (meCbl)) as well as other metabolites associated with one-carbon metabolism (thymidine monophosphate (dTMP) or glutathione) (Fig. 1B) failed to liberate cells (Fig. S4J and K). These results suggest that D-serine impacts the folate cycle rather than the methionine cycle in one-carbon metabolism to prevent growth of neuroblastoma cells.

As neurons and astroglia share a common developmental origin, we further tested whether glial tumor cells also show vulnerability to D-serine. Glioblastoma is the most common malignant brain tumor in adults, whose survival rate is low despite advances in surgical and medical neuro-oncology(Bent et al., 2023; Delgado-López and Corrales-García, 2016). Among human glioblastoma cell lines (U87, U251, SF126), U251 cells were the most sensitive to D-serine treatment (Fig. 3C). Supplementation with glycine and formate restored proliferation of U251 (Fig. 3D), and 5,10-meTHF recovered the vulnerability to D-serine, albeit very mildly (Fig. 3E), supporting the significance of one-carbon metabolism in growth of glioblastoma cell lines too. To further test the anti-proliferative effect of D-serine in the tumor

microenvironment, we made an organotypic brain slice culture from mice with orthotopic xenografts of glioblastoma cells expressing Venus fluorescence(Tamura et al., 2019). Brain slices of mice implanted with U87 cells in the striatum were cultured *ex vivo* for 7 days in serine/glycine-free media containing D-serine or vehicle. D-serine strikingly suppressed expansion of U87 cells with Venus fluorescence compared to the control treatment, even in *ex vivo* tumor culture (Fig. 3F and G). Since glioma stem cells (GSCs) in the glioblastoma have self-renewal and tumor-initiating capacity and cause cancer recurrence(Gimple et al., 2022; Tang et al., 2021), we wondered whether GSCs also have similar vulnerability to D-serine. *In vitro*, D-serine reduced viability of cell lines for GSCs (hG008 and hG020), established from human glioblastoma specimens[25], in a dose-dependent manner with greater efficacy to the hG008 line (Fig. 3H). This growth defect in hG008 cells induced by D-serine was rescued by supplementation with glycine and formate, as in neuroblastoma and glioblastoma cells (Fig. S4L). hG008 cells have a sphere-forming capacity[23], and we also observed D-serine-induced reduction of sphere diameters of hG008 cells cultured under the sphere-forming conditions (Fig. 3I). Moreover, in brain slices of mice with orthotopic xenografts of hG008 cells expressing Venus fluorescence, D-serine significantly inhibited growth and invasiveness of hG008 cells (Fig. 3J and K). Thus, brain tumor cells showed consistent vulnerability to D-serine via inhibition of one-carbon metabolism.

D-serine induces apoptosis by interfering with one-carbon metabolism in neuroprogenitor cells

Neural stem cells have similar characteristics to neural tumor cells with high proliferative capacity(Reya et al., 2001). To test whether D-serine also affects immature neurons, we made a primary culture of neuroprogenitor cells (NPCs) from telencephalon in E14 mice in serine-free Neurobasal medium, treated with D- or L-serine from DIV1. At DIV7, L-serine treatment significantly increased the number of neurons with a condensed neurites compared to vehicle-treated neurons. In contrast, D-serine-treated culture had fewer number of neurons with sparse neurites, suggesting that D-serine has a negative impact on maturation of NPCs (Fig. 4A). Furthermore, D-serine activated cleavage of caspase-3 dose-dependently in Nestin-positive NPCs and Tubb3+ developing neurons 48 h after treatment, whereas L-serine had no effect (Fig. 4B-D, Fig. S5A-C). In contrast, vesicular glutamate transporter 2 (vGlut2)-positive mature excitatory neurons, glutamate decarboxylase-67 (Gad67)-positive mature inhibitory neurons, and glial fibrillary acidic protein (Gfap)-positive glial cells did not undergo apoptosis under D- or L-serine treatment (Fig. 4B and Fig. S5D and E), suggesting that mature neurons and astrocytes are resistant to D-serine. Consistently, D-serine treatment at DIV7 did not activate cleavage of caspase-3 or reduce proliferation of neurons (Fig. 4E and F). Susceptibility of NPCs was pronounced in the presence of D-serine, but was not caused by other D-amino acids, such as D-aspartate, D-alanine, or D-proline (Fig. S6A), which can be detected in mammalian intestinal bacteria(Gonda et al., 2023). As D-serine is a coagonist of NMDA receptors(Mothet et al., 2000; Wolosker and Balu, 2020), we further tested whether D-serine neurotoxicity involves NMDA receptors(McNamara and Dingledine, 1990). Blockade of Ca^{2+} influx through NMDA receptors by a non-competitive NMDA antagonist, MK-801, or of D-serine-binding to the receptors by 5,7-dichlorokynurenic acid (DCKA) did not attenuate D-serine neurotoxicity (Fig. S6B and C). Also, inhibition of the receptor's downstream signal by *N*-nitro-L-arginine methylester (L-NAME) or an antioxidant (glutathione) did not affect enhanced cleavage of caspase-3 by D-serine (Fig. S6D and E). Thus, our findings suggest that apoptosis triggered by D-serine in NPCs does not mediate NMDA receptors. To test whether apoptosis triggered by D-serine involves amino acid metabolism, we supplemented NPCs treated with D-serine from DIV1 with various L-amino acids or glycine. As expected, among L-amino acids and glycine, L-serine specifically and dose-dependently inhibited cleavage of caspase-3 caused by D-serine (Fig. 4G and H), which is consistent with competitive mitochondrial transport of serine enantiomers (Fig. 2F). Moreover, similar to the observation that 5,10-methylene THF rescued neural tumor cell growth (Fig. S4I), 5,10-methylene THF restored D-serine-induced cleavage of caspase-3 in NPCs (Fig. 4I), suggesting that D-serine interferes with L-serine functions, such as its role in one-carbon metabolism.

To further rule out alternative mechanisms, we examined whether D-serine disrupts L-serine-mediated lipid synthesis. During the neuronal development, NPCs require L-serine to synthesize

membrane sphingolipids and phospholipids that support cellular expansion and neurite elongation (Fig. S7A). A comparative lipidomic study using NPCs revealed that D-serine treatment increased phosphatidylserine, but not sphingolipids or other phospholipids (Fig. S7B and C). To test whether D-serine is incorporated into phosphatidylserine, we extracted membrane lipids, hydrolyzed phosphatidylserine using phospholipase D (PLD) to release serine, and quantified serine enantiomers using 2D HPLC (Fig. S7D and E). Phosphatidylserine extracted from NPCs cultured without D-serine harbored only L-serine, but supplementation with D-serine significantly increased phosphatidyl-D-serine and decreased phosphatidyl-L-serine (Fig. S7F). This effect was abolished by co-supplementation with L-serine (Fig. S7F). However, exogenous phosphatidyl-L-serine failed to rescue D-serine-induced apoptosis (Fig. S7G), indicating that composition of membrane phosphatidyl-serine is not the primary cause of cell death. Together, these results demonstrate that D-serine impairs the survival of immature neural cells not by modulating neurotransmission or lipid metabolism, but by disrupting one-carbon metabolism through competition with L-serine.

Enantiomeric shift of serine metabolism during neural development

Serine metabolism is fundamental to multiple cellular functions and crucial for neural development. To gain a functional overview of how serine chirality contributes to these processes, we monitored serine enantiomers and glycine using the 2D HPLC system. L-serine levels in the mouse cerebral cortex showed a gradual increase during embryonic development, dropped at birth, and remained at a concentration above 500 nmol/g thereafter (Fig. 4J). As glycine synthesis depends in part on L-serine, glycine showed a similar trend to L-serine in embryo and maintained levels above 800 nmol/g after birth (Fig.4J). On the other hand, D-serine was trace during the embryonic stage, but increased gradually after birth. Therefore, the D/L-serine ratio exhibited a steady increase after birth and reached 0.4 in mature mouse brain (Fig. 4J). The dynamics of serine enantiomers during the brain development is corroborated by transcriptional profiles associated with serine chial metabolism. Bulk RNA-seq data of developing neurons derived from mouse embryonic stem cells (ESC)(Hubbard et al., 2013) or human inducible pluripotent stem cells (iPSC)(Burke et al., 2020) in public databases showed that diverse transcriptions found in the phosphorylated pathway of L-serine synthesis (PHGDH, PSAT1, and PSPH), one-carbon metabolism (SHMT1/2, MTHFD1/2, and MTHFD1/2L), and nucleic acid synthetic pathway (DHFR, TYMS, MTHFS) decrease along with the neuronal maturation (Fig. S8A and B). In contrast, D-serine-synthetic enzyme SRR increases after days *in vitro* 7 (DIV7) in ESC-derived neurons and NPC/Rosetta cells (DIV14-21) in human iPSC-derived neurons. Subunits of NMDA receptors, including Grin1/GluN1, to which D-serine or glycine binds, are expressed in matured neurons after DIV16 of mouse ESC-derived cells (Fig. S8A) or those at DIV49 of human iPSC-derived cells (Fig. S8B). Alterations of serine metabolism during development were further supported by single-cell RNA-seq performed by Bella et al.(Bella et al., 2021), which provides crucial information about the trajectory of differentiating cells and cell type-specific transcriptional profiles during mouse brain development *in vivo*. Uniform manifold approximation and projection (UMAP) illustrates that Sox2+ neural progenitor cells (cluster 1, 7, 9, and 11) express L-serine synthetic enzymes (Phgdh, Psat1, Psph) and folate cycle enzymes (Tyms, Mthfd1, Dhfr) as well as a proliferation marker gene Mki67 (Fig. 4K and Fig. S8C and D). Apoe+ and Aldh1l1+ astrocytes (cluster 7) also express L-serine synthetic pathways, whereas Tubb3+ mature neurons (cluster 0, 2, 3, 4, 5, 8, 12, 13, 15, 16, 19, 22) do not express serine synthetic enzymes (Fig. 4K and Fig. S8C and D). Tubb3+ neurons weakly express Srr at P4 but not E10 (Fig. S8E). These transcriptional profiles suggest that reduction of L-serine biosynthesis during neural development accompanies inactivation of the folate cycle and one-carbon metabolism, and that mature neurons start to synthesize D-serine. Given that the folate cycle and one-carbon metabolism, essential for nucleic acid biosynthesis, are the metabolic signature of cell proliferation, NPCs lose their metabolic activity for proliferation in the embryonic stage but instead develop the capacity for neurotransmission during the postnatal development. Although we found that D-serine inhibits L-serine-dependent one-carbon metabolism, its endogenous production is minimal in neural stem/progenitor cells and increases only after the onset of neuronal maturation, coinciding with the upregulation of Srr. Thus, D-serine is unlikely to play a direct role in regulating

proliferative metabolism during early neurodevelopment. Rather, its selective synthesis in post mitotic neurons appears metabolically rational, aligning with their shift from proliferation to neurotransmission.

Discussion

We found that D-serine competes with mitochondrial transport of L-serine, thereby limiting substrate availability for Shmt2 and suppressing one-carbon metabolic flux. This metabolic interference leads to reduction of glycine and formate, as well as downregulation of downstream pathways including polyamine synthesis. Functionally, under L-serine limited conditions, D-serine suppresses the proliferation and survival of immature neural cells, independent of NMDA receptor activation. Moreover, we demonstrated that endogenous D-serine production increases postnatally in tandem with neuronal maturation, whereas early progenitor cells remain devoid of D-serine synthetic enzyme. These findings highlight a previously unrecognized, stereoselective regulation of cellular metabolism by D-serine, and provide a rationale for its selective synthesis in mature neurons where proliferative metabolic activity is no longer required.

In the central nervous system, L-serine increases during fetal development and declines rapidly after birth, while D-serine increases only after birth and reaches the mature levels within a few weeks (Fig. 4J). This postnatal increase of D-serine is consistent with a previous report in rats(Hashimoto et al., 1993) and can be explained by a gradual increase of Srr after birth in mouse glutamatergic neurons (Fig. S8A and E) or forebrain tissue(Miya et al., 2008). In the mature brain, the majority of Srr is restricted to neurons(Balu et al., 2014; Miya et al., 2008), which coincides with our view that D-serine synthesis is a sign of neuronal maturation. In contrast, PHGDH is not expressed in neurons, but is confined to astrocytes in mature brain(Yang et al., 2010). This astrocyte-specific expression of the L-serine synthetic enzyme accords with our findings that a set of genes encoding enzymes for L-serine synthesis and one-carbon metabolism are downregulated in mature neurons, but confined to a cell population with mature astrocyte markers (Fig. 4K and S8). Given that astrocytes require one-carbon metabolism for proliferation and that neurons prioritize neurotransmission, such cell-type specific and enantio-selective serine metabolism in the matured brain appears to be a reasonable metabolic compartmentalization. Indeed, loss of D-serine synthesis does not trigger developmental abnormalities(Miya et al., 2008), but causes functional or structural abnormalities in mature neurons(Balu et al., 2012; Basu et al., 2009; Horn et al., 2017; Sultan et al., 2015). Furthermore, supplementation with D-serine in the neonatal brain enhances functional development of forebrain neurons(Nomura et al., 2016). Therefore, it is likely that D-serine does not promote differentiation of NPCs, but contributes to functional maturation of differentiated neurons.

While D-serine is important for functional maturation of neurons as well as excitatory neurotransmission through NMDA receptors(Basu et al., 2009; Horn et al., 2017; Mothet et al., 2000), D-serine has an inhibitory effect on proliferation and triggers apoptosis in NPCs and other immature cells (Fig. 3 and 4). Extracellular D-serine is a classic trigger of excitotoxicity in neurons(Patel et al., 1990; Shleper et al., 2005), whereas it induces intracellularly necrosis/apoptosis in renal tubular cells at high doses(Kaltenbach et al., 1979; Williams and Lock, 2004). Excitotoxicity of D-serine has been reported in mature neurons in ischemic or neurodegenerative diseases and mediates NMDA receptors (Inoue et al., 2008; Mustafa et al., 2010; Sasabe et al., 2007; Shleper et al., 2005). In contrast, the D-serine toxicity, which we observed in neural culture, occurs only in immature neurons, and can be rescued by L-serine or intermediates of the one-carbon metabolism, but not by inhibitors of NMDA receptors or their downstream signals (Fig. 4G-I and S6). The latter toxicity reported in kidneys mediates hydrogen peroxide generated through degradation of D-serine by a D-serine catabolic enzyme, D-amino acid oxidase, plentiful in kidneys(Maekawa et al., 2005). Nonetheless, D-amino acid oxidase is not expressed in neurons or in the forebrain(Gonda et al., 2022). Furthermore, as we could not find protective effects by an antioxidant against D-serine toxicity in immature neurons (Fig. S6E), involvement of oxidative stress by hydrogen peroxide is unlikely. Thus, D-serine toxicity observed in this study does not appear mediated by mechanisms previously reported. Importantly, Okada et al., suggests that renal tubular toxicity by D-serine can be ameliorated by L-serine(Okada et al., 2017). Although the authors did not demonstrate involvement of one-carbon metabolism in D-serine toxicity in the kidneys, their observation could be associated with our findings that D-serine functionally competes with L-serine (Fig. 4H).

We show that D-serine attenuates cell proliferation by inhibiting one-carbon metabolism (Fig. 3). D-serine concentration required to inhibit cell proliferation is greater than physiological concentration (~300

μM), therefore it is unlikely that physiological level of D-serine determines cell fate. However, it is important to understand that concentration of D-serine increase over the brain development that interferes efficient L-serine metabolic process. Since proliferative cells require one-carbon units for nucleotide synthesis and methylation (Fig. 1B), one-carbon metabolism is crucial for both developmental and proliferative tissues(Ducker and Rabinowitz, 2017). As we observe that immature cells are susceptible to D-serine (Fig. 4), demand for one-carbon units is highest in fetal development(Ducker and Rabinowitz, 2017). Indeed, in humans, deficiency of L-serine or folate, which receives one-carbon units from L-serine, leads to congenital defects in the central nervous system(Acuna-Hidalgo et al., 2014; Beaudin and Stover, 2009). Supply of one-carbon units from L-serine has both cytoplasmic and mitochondrial branches in one-carbon metabolism (Fig. 1B), but the mitochondrial pathway is critical in embryonic development(Ducker and Rabinowitz, 2017; MacFarlane et al., 2008). Therefore, transport of L-serine, generated in the cytoplasm, into mitochondria appears to be a critical step for cellular proliferation during development. A seminal study by Kory et al. has shown that sideroflexin 1, a multipass inner mitochondrial membrane protein, and its homologs mediate L-serine transport to mitochondria(Kory et al., 2018). Notably, they show *in vitro* that D-serine competes with L-serine transport through sideroflexin 1. Together with our results from an *in vivo* L-serine competition assay (Fig. 2F), D-serine may compete with general L-serine transport to mitochondria through transporters, such as sideroflexin homologs. In addition, *de novo* serine synthesis and mitochondrial one-carbon pathway are required for the proliferative phenotype in a large variety of human cancers(Jain et al., 2012; Labuschagne et al., 2014; Lee et al., 2014; Lewis et al., 2014; Nilsson et al., 2014). Therefore, the broad anti-proliferative effect of D-serine on neural tumor cells (Fig. 3) supports our idea that D-serine inhibits the mitochondrial one-carbon pathway. Since cancer genetics indicate two pathways not targeted by existing therapies, de novo serine synthesis and mitochondrial one-carbon metabolism(Ducker and Rabinowitz, 2017; Newman and Maddocks, 2017), inhibition of L-serine transport to mitochondria, such as by potent D-serine derivatives, to disconnect these two pathways might be a reasonable target for development of cancer therapeutants.

Neuronal metabolism exhibits the unique property of serine isomerization to adapt to functional maturation (Fig. 4). Consequently, mature cerebrum contains sub-millimolar levels of D-serine, which account for a quarter of total serine in the cerebrum and are about 100-times higher than blood levels(Miyoshi et al., 2009). This active stereo-conversion of serine in the cerebrum is unique to mammals among vertebrates(Nagata et al., 1994), implying that neurophysiological functions of D-serine are inseparable from the functional evolution of the cerebrum in higher vertebrates. Indeed, whereas either D-serine or glycine are required to activate NMDA receptors, D-serine binds to the GluN1 subunit of NMDA receptors with higher affinity than does glycine(Furukawa and Gouaux, 2003) and also has an inhibitory effect on the GluN3 subunit by competing with glycine(Chatterton et al., 2002). Therefore, extracellular D-serine appears to be evolutionarily important as a neurotransmitter, with different properties than glycine. On the other hand, the inhibitory function of intracellular D-serine against mitochondrial one-carbon metabolism (Fig. 1 and 2) may be an evolutionarily inherited trait from the biological ancestors of mitochondria, bacteria(Archibald, 2015). Notably, bacteria depend on one-carbon metabolism for their growth, and D-serine attenuates bacterial growth by inhibiting L-serine metabolism(Cosloy and McFall, 1973). Therefore, bacterial sensitivity to D-serine may reveal a common pathway for inhibition of mitochondrial one-carbon metabolism by D-serine. Given that neurons do not express enzymes for mitochondrial one-carbon metabolism upon maturation (Fig. S8), evolutionary acquisition of neurophysiological functions of D-serine without cytotoxicity may be due to the fact that mature neurons are not proliferative and do not depend on this conserved metabolic feature of mitochondria. While complete understanding of the significance of serine stereo-conversion in the developmental brain will require further studies to illuminate neurogenesis under spatio-temporally controlled D-serine, our findings provide a basis to understand the significance of maintaining serine enantiomer balance in the central nervous system.

Materials and Methods

Animals

All animal experiments were approved by the institutional Animal Experiment Committee and conducted in accordance with Institutional Guidelines on Animal Experimentation at Keio University. C57BL/6Jcl mice were purchased from CLEA Japan (Tokyo, Japan). ICR mice were from Charles River Laboratories (Wilmington, MA, USA). Female BALB/c nude mice (BALB/cSlc-nu/nu) were from Japan SLC (Shizuoka, Japan). Mice were raised in 12 h light and dark cycle with free access to food (CE-2, CLEA Japan) and water in the specific pathogen-free environment.

Antibodies

Rabbit polyclonal antibodies to cleaved caspase-3 (5A1E) and to GAPDH (14C10) were purchased from Cell Signaling Technologies (Danvers, MA, USA). Mouse monoclonal antibodies to GFAP (Z0334), vGLUT2 (8G9.2), and GAD67 (1G10.2) were from Agilent Technologies (Santa Clara, CA, USA), Abcam (Cambridge, UK), and Merck Millipore (Darmstadt, Germany), respectively.

Cell culture and proliferation assay

NPCs and primary cultured astrocytes (PCAs) were prepared as follows. Telencephalon tissues from ICR mice were dissected at the embryonic day 14, treated with papain, and disassembled by pipetting. The cell suspension was passed through a 40-μm filter, centrifuged, and resuspended in a Neurobasal medium without serine (NB-S). NB-S was manufactured by Research Institute for the Functional Peptide (Yamagata, Japan) based on the concentration of each chemicals in Neurobasal media (ThermoFisher: 21103049) described in the technical resources at ThermoFisher. NPCs were cultured in NB-S supplemented with 2% B-27 supplement (ThermoFisher, Waltham, MA, USA), 1% Penicillin-streptomycin solution (ThermoFisher), and 1% GlutaMAX supplement (ThermoFisher). For PCAs, NPCs were differentiated into astrocytes within 7 days by changing the medium to D-MEM (high glucose) (Fujifilm Wako, Tokyo, Japan) supplemented with 10% FBS (A5256701, ThermoFisher) and 1% Penicillin-Streptomycin at 24 h *in vitro*.

Neuroblastoma (Neuro2a, F11, NSC34, and SHSY5Y) and glioma (U87, U251, SF126) cell lines were cultured in MEM supplemented with 10% dialyzed FBS (S-FBS-NL-065, SERENA Europe GmbH, Brandenburg, Germany), 5 mM D-glucose, 65 μM sodium pyruvate, 1 × MEM vitamin solution (ThermoFisher), 2 mM L-glutamine, 0.15 mM L-proline, 0.15 mM L-alanine, 0.15 mM L-aspartic acid, 0.15 mM L-glutamic acid, and 0.34 mM L-asparagine (-SG media) as described in Tajan et al.(Tajan et al., 2021), unless otherwise noted. Proliferation of NPCs, PCAs, and cancer cell lines was analyzed with Cell Counting Kit-8 in accordance with the manufacture's protocol (Dojindo, Kumamoto, Japan).

Western blot

NPCs were harvested in a lysis buffer [50 mM Tris-HCl, pH 7.4, 150 mM NaCl, 20 mM ethylenediaminetetraacetate (EDTA), 1% TritonX-100, protease inhibitor cocktail (Sigma-Aldrich, St. Louis, MO, USA)]. Protein concentration was analyzed with a BCA assay kit (ThermoFisher), and 20-80 μg of protein were subjected to SDS-PAGE. Then, proteins were transferred to the PVDF membranes and blocked with 10% skim milk in PBST. Proteins were detected with anti-cleaved caspase-3 antibody or ant-GAPDH antibody (Cell Signaling Technology, MA, USA), and HRP-conjugated secondary antibodies (Jackson ImmunoResearch Laboratories, PA, USA).

Metabolomics

Cells were washed twice with 10 mL of PBS(-). The PBS(-) was aspirated, and 1 mL of MeOH containing internal standards was added to the dish. The dish was left for 10 min, and a sample solution was obtained and transferred to a tube. For metabolite extraction, the tube was vortexed and subsequently centrifuged at 20,380×g for 10 minutes at 4 °C (MDX-310, TOMY Seiko, Tokyo, Japan). The 150 μL of supernatant was transferred to another tube and dried by centrifugation at 1,600 rpm (366×g) for 90 min at room temperature (VC-96W, Taitec, Saitama, Japan). Then, 10 μL of 90% MeOH were added, 30 μL

of H_2O were added and mixed, and then the tube was centrifuged at 20,380×g for 10 minutes at 4 °C. The 20 μL of supernatant were transferred to a vial and injected into the LC-MS system.

The LC-MS instrument has previously been described in detail(Fuse et al., 2020). Briefly, an Agilent Technologies 1290 Infinity LC system and a G6230B time-of-flight MS (TOF–MS) (Agilent Technologies, Santa Clara, CA, USA) were used. Each sample was analyzed in positive and negative modes. Conditions for the analysis in positive mode were set as described previously, with slight modification(Tomita et al., 2018). The temperature of the LC columns was set at 40 °C. For negative mode, the chromatographic separation was performed using an ACQUITY HSS T3 column (2.1 i.d. × 50 mm, 1.8 μm; Waters, Milford, MA, USA) at 30 °C. The mobile phase, consisting of solvent A (0.1% formic acid in water) and solvent B (acetonitrile), was delivered at a flow rate of 0.3 mL/min. In this study, 50–1,200 m/z was used for the MS setting in negative mode.

Data processing from raw LC-MS data to produce a data matrix including metabolite concentration (sample × metabolite) was described previously(Pang et al., 2021). Data analyses were performed using MetaboAnalyst (ver. 5.0, https://www.metaboanalyst.ca/)(Pang et al., 2021) to produce volcano plots and to conduct pathway analysis and pattern searches. Overall data profiles were visualized using MeV TM4 (ver. 4.9.0, https://sourceforge.net/projects/mev-tm4/).

Quantification of glycine and serine enantiomers

Glycine and serine enantiomers in cell-cultured media or brain tissues were measured using two-dimensional HPLC, as previously described(Gonda et al., 2023; Ishii et al., 2018). Briefly, samples were mixed with 9 volumes of MeOH and centrifuged to remove protein depositions. Supernatants were spin-dried and resuspended in Milli-Q water. Resuspensions were resuspended in 200 mM sodium borate, and then derivatized with 4-fluoro-7-nitro-2,1,3-benzoxadiazole (NBD-F). NBD-conjugated amino acids were injected into a two-dimensional HPLC system (NANOSPACE SI-2 series, Shiseido, Tokyo, Japan), separated on an octadecylsilyl column (Singularity RP18, 1.0 mm inner diameter (ID) × 250 mm) (designed by Kyushu University and KAGAMI Co. Ltd., Osaka, Japan), and further separated into enantiomers on a Pirkle-type enantioselective column (Singularity CSP-001S, 1.5 mm ID × 250 mm) (designed by Kyushu University and KAGAMI). Fluorescence of NBD-amino acids was detected at 530 nm with excitation at 470 nm. D- and L-serine peak in a chromatogram were detected and standard curve was drawn by the peak height of those standards. The absolute amount of D- and L-serine were calculated by standard curve method.

Quantification of formate in the culture media

Formate concentration in the culture media was measured using Enzychrom Formate assay kit (BioAssay Systems) according to the manufacturer's protocol.

SHMT2 activity assays

The SHMT2 gene was cloned from cDNA of HeLa cells using primers 5'-GCCCATATGGCCATTCGGGCTCAGCAC-3' (forward) and 5'-GCCCTCGAGATGCTCATCAAAACCAGGCA-3' (reverse) and subcloned into the pET41a vector (Novagen, WI, USA) at restriction enzyme sites of NdeI and XhoI. C-terminally hexahistidine (His_6)-tagged human SHMT2 was purified as follows. *E. coli* BL21 (DE3) pLysS-competent cells were transformed with pET41-SHMT2, cultured at 37 °C in Luria-Bertani medium containing 20 μg/mL kanamycin, and grown until the OD600 reached 0.6-0.7. Isopropyl β-D-thiogalactopyranoside was added to a final concentration of 0.5 mM, and culturing was continued for an additional 24 h at 20°C. Harvested cells were resuspended in 20 mM sodium phosphate buffer (pH7.4) containing 500 mM NaCl and protease inhibitors (Nacalai Tesque, Kyoto, Japan), and sonicated using a Sonifier 250 instrument (Branson, CT, USA). Lysed cells were centrifuged at 20,000 × g for 10 min at 4 °C, and imidazole was added to the supernatant to a final concentration of 100 mM. The supernatant was applied to a His SpinTrap column (Cytiva, Tokyo, Japan). The column was washed with 20 mM sodium phosphate buffer (pH7.4) containing 500 mM NaCl and 100 mM imidazole. and recombinant protein was eluted with 20

mM sodium phosphate buffer (pH7.4) containing 500 mM NaCl and 500 mM imidazole. Protein fractions were buffer-exchanged into 50 mM Tris-HCl (pH8.0) containing 100 mM NaCl and 10% glycerol using an Amicon Ultra-0.5 centrifugal filter 10K device (Merck Millipore, Darmstadt, Germany).

SHMT2 activity was determined by measuring the production of glycine. The reaction mixture (150 µL) contained 50 mM HEPES-NaOH (pH8.0), 0.2 mM L-serine, 50 µM PLP, 50 µM THF, 1 mM dithiothreitol, and recombinant SHMT2 (2 µg). D-serine was added at concentrations varying from 0.1 to 0.4 mM. The reaction mixture was incubated at 37 °C for 10 min, and then 600 µL of MeOH were added to terminate the reaction. Glycine was derivatized with ortho-phthaldialdehyde (OPA) and *N*-tert-butyloxycarbonyl-L-cysteine (Boc-L-Cys), and an aliquot (10 µL) was injected into an LC-4000 Series HPLC system (Jasco Corp., Tokyo, Japan) equipped with a Mightysil RP-18GP column (150 × 4.6 mm i.d.; Kanto Chemical Co., Tokyo, Japan). A gradient of solvent A (50 mM sodium acetate buffer, pH 6.0) and solvent B (acetonitrile) was applied at a flow rate of 1 mL/min. A linear gradient was applied for 35 min from 10% to 21% solvent B for glycine analysis. Excitation and emission wavelengths for fluorescence detection were 344 nm and 443 nm, respectively.

L-serine transport assay in semi-permeabilized cells

Neuro2A cells were seeded on poly-D-lysine coated 24-well-plate, cultured for 3 days, and subjected to the transport assay. Transport of L-[^{3}H]serine was examined in semi-permeabilized cells. For plasma membrane permeabilization, cells were treated with saponin, an agent that permeabilizes the plasma membrane but leaves membranous organelles intact(Klepinin et al., 2016; Kuznetsov et al., 2008). The optimized saponin concentration and treatment time were verified by optical microscopy. Transport assays were performed as described previously(Lee et al., 2022; Wiriyasermkul et al., 2012) with some modifications. After washing the cells with 37^{o}C pre-warmed Dulbecco's Phosphate Buffered Saline (DPBS) with 1 mM $MgCl_2$ and 0.25 mM $CaCl_2$, they were incubated for 6 min in the same buffer containing 40 µg/mL saponin (Fujifilm) for plasma membrane permeabilization. Transport of 10 µM L-[^{3}H]serine (100 Ci/mol; Moravek Biochemicals, Brea, CA, USA) with or without D-serine (at indicated concentrations) was measured for 10 min in the same buffer including saponin. After terminating the reaction and cell lysis, an aliquot of the lysate was used to measure protein concentration by BCA protein assay (Takara Bio). The lysate was mixed with OptiPhase HiSafe 3 (PerkinElmer), and radioisotope activity was monitored by LSC-8000 β-scintillation (Hitachi, Tokyo, Japan). Data shown in the figures were those subtracted from uptake values at 0 min. Kinetics of inhibition was fitted to the Nonlinear Regression: dose-response – inhibition model of GraphPad Prism 8.4.

RNA-sequence and analysis

Neuro2a cells were cultured in D-MEM with 10% FBS. The medium was changed to D-MEM(-SG) including 10% dialyzed FBS with or without 5 mM D-serine. Cells were harvested in Trizol after 18 h of incubation at 37 °C in a CO_2 incubator. RNA was extracted from cells according to the manufacture's protocol. mRNA libraries of each sample were prepared using a TruSeq Stranded mRNA library Kit (Illumina, San Diego, CA) according to the manufacturer's protocol and paired end sequences were read by NovaSeq (Illumina). Adapter sequences were trimmed from raw sequences with Trim Galore (https://www.bioinformatics.babraham.ac.uk/projects/trim_galore/) and trimmed sequences were mapped to the mouse genome (GRCm38/mm10) using HISAT2 (https://daehwankimlab.github.io/hisat2/). Aligned sequences were counted using FeatureCounts (https://subread.sourceforge.net/). Differentially expressed genes were identified by DESeq2 (https://bioconductor.org/packages/release/bioc/html/DESeq2.html). Gene Set Enrichment analysis was performed to find enriched biological pathways using ClusterProfiler (https://bioconductor.org/packages/release/bioc/html/clusterProfiler.html) with the following settings: pAdjustMethod = fd, pvalueCutoff = 0.05, minGSSize = 10, maxGSSize = 400.

Glioma stem cell culture

hG008 and hG020 cells, established from human glioblastoma specimens(Fukaya et al., 2016), were cultured in Ultra-Low attachment cell culture flasks (Corning, Kennebunk, ME, USA) in a medium, in which ingredients were manually mixed in MEM to make DMEM/Ham's F-12 with HEPES without serine and glycine (D/H-SG). The D/H-SG medium was supplemented with 2% B-27 (ThermoFisher), 20 ng/mL recombinant human fibroblast growth factor-basic (PeproTech, Rocky Hill, NJ, USA), 20 ng/mL recombinant human epidermal growth factor (PeproTech), 1000 units/mL recombinant human leukemia inhibitory factor (Nacalai Tesque, Kyoto, Japan), and 1 unit/mL heparin. Sphere formation of hG008 cells (1×10^4 cells/well in 96-well plates with ultra-low attachment surface, Corning) was observed using EVOS M5000 (ThemoFisher) and the maximum diameter of spheres in each well was measured after 7 days of culture.

Ex vivo cancer growth assay

U87 and hG008 cells were transduced with the lentiviral vector CSII-EF-ffLuc, and single-cell suspensions were cultured in 96-well plates. Xenografts were implanted in the brain of female BALB/c nude mice as described previously[25]. Briefly, mice were implanted with Venus fluorescence-labeled U87 (5×10^5 cells/2 μL in PBS) or hG008 (1×10^5 cells/2 μL in PBS) under anesthesia on a stereotaxic apparatus (Narishige Scientific Instrument Lab, Tokyo, Japan). Mice were sacrificed after 6 days (U87) or 35 days (hG008) of implantation. Mouse brains were dissected, cut into a 200-μm slices, and cultured on the Millicell cell culture inserts (Millipore-Sigma, Burlington, MA) placed on a 35 mm glass-bottom dish filled with D/H-SG medium with or without 100 mM D-serine. Fluorescence images were taken with a FV3000 (Olympus, Tokyo, Japan) on days 0 and 7 and analyzed with Image J software (https://imagej.nih.gov/ij/index.html).

Statistics

No statistical methods were used to predetermine sample size. Blinding was not performed. No randomization was used. Prism 10 (GraphPad Software) was used for data plotting and statistical analyses. Statistical significance was determined with unpaired t-tests to compare two groups, or one-way analysis of variance (ANOVA) for multiple comparisons when data were normally distributed and had equal variance. ANOVA was followed by Dunnett's post-hoc test (comparison to control) or Tukey's post-hoc test (comparisons among samples).

Data Availability

RNA-seq data are available at Gene Expression Omnibus (GEO) with accession number GSE268106.

Acknowledgements

We thank Kenji Hamase and Masashi Mita for technical support on chiral amino acid analysis and Steven D Aird for editing the manuscript. This study was supported by the Grants-in-Aid for Scientific Research (KAKENHI) 15K19497 (MS), 17J10213 (MS), 22K19408 (JS), Keio Gijuku Fukuzawa Memorial Fund for the Advancement of Education and Research (JS), and Keio Program for the Promotion of Next Generation Research Projects Type A (JS).

Figures

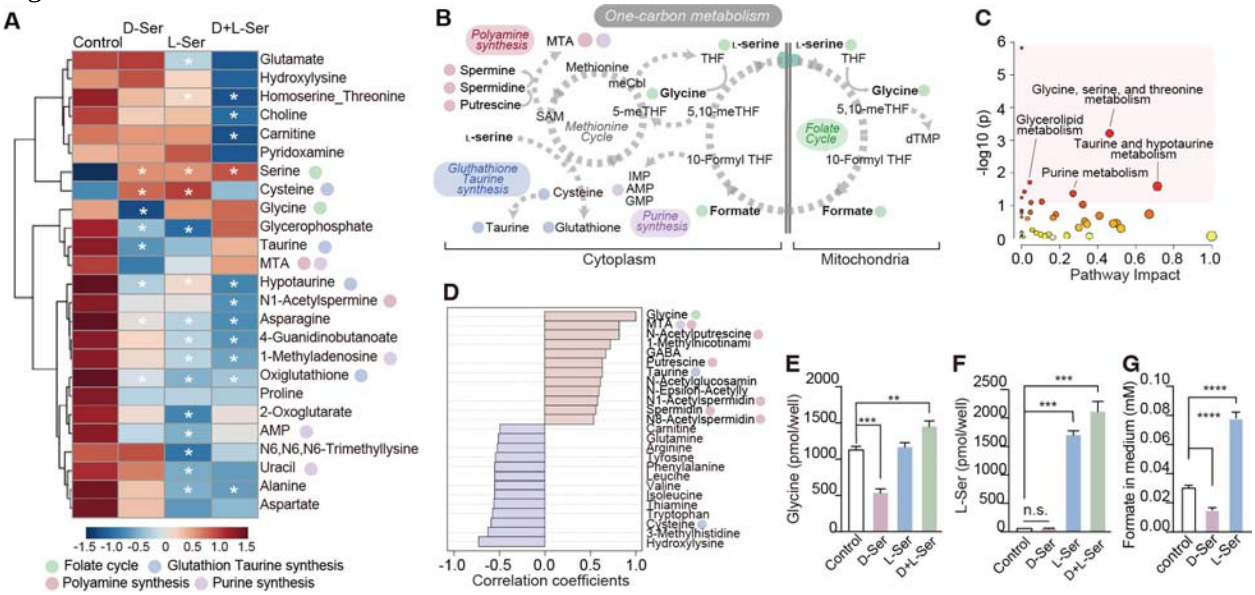

Fig. 1 D-serine inhibits one-carbon metabolism

A. A heatmap shows top 25 metabolites in PCNs altered by treatment with D- and/or L-serine in the metabolomic analysis (n = 3). **B**. Major metabolites in the one-carbon metabolism. **C.** KEGG metabolic pathways enriched in D-serine treated cells compared to vehicle treated cells. **D.** Pearson's correlation coefficients between glycine and other metabolites. Top 25 metabolites positively (red) and negatively (blue) correlated with glycine are shown. **E, F**. Concentrations of glycine (**E**) and L-serine (**F**) in PCNs were quantified using HPLC (n = 4). **G.** Concentrations of formate in the culture media of PCNs treated with 2 mM D- or L-serine (n = 4). Data are presented as the mean ± s.e.m. (**E, F,** and **G**). Statistical significance was evaluated by one-way ANOVA followed by Dunnett's post hoc-test (**E, F,** and **G**). *p < 0.05 (**A**). Data are the representative of two independent experiments.

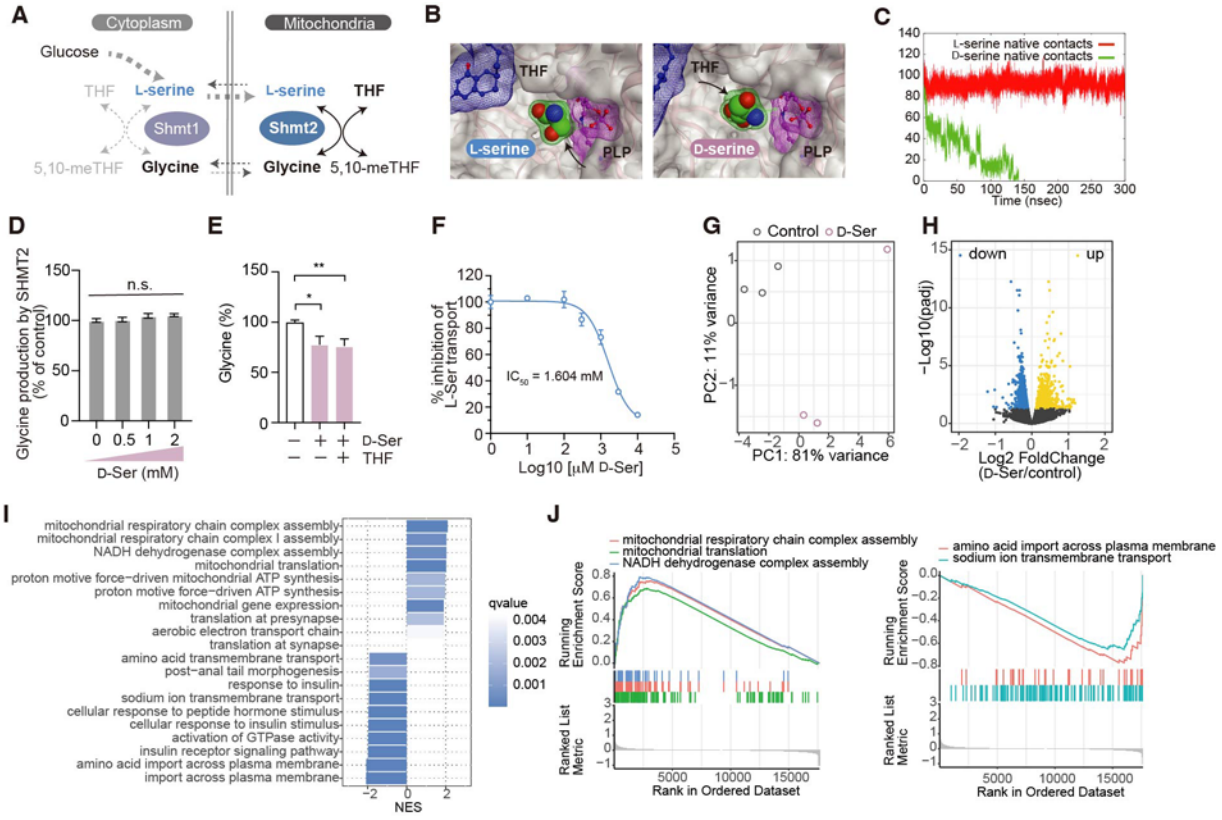

Fig. 2 D-serine inhibits cytoplasmic L-serine transport to mitochondria

A. L-serine/glycine transport and conversion across cytoplasm and mitochondria in one-carbon metabolism. **B.** Binding sites of D- (right) or L-serine (left), THF, and pyridoxal phosphate (PLP) in the ligand-bound SHMT2 complex systems. Arrows indicate carbon atoms on serine enantiomers that transfer to THF. **C.** Time series variation of the number of contact atoms within the distance cutoff of 7.0 Å from D- or L-serine observed at the initial structure. **D.** SHMT2 enzymatic activity determined by glycine production is shown as percent of control (with no D-serine) (n = 3). **E.** Relative concentrations of glycine in NPCs treated with or without 2mM D-serine and/or 50 μM THF. **F**. Inhibition of mitochondrial L-serine transport by D-serine was examined in semi-permeabilized cells (n = 4). **G.** A PCA plot shows RNA-seq results from cells treated with D-serine (pink) or control (gray). **H**. A volcano plot indicates differentially expressed genes in cells treated with D-serine vs controls. Gene expressions with adjusted *p*-values < 0.05 are highlighted in yellow (up) or blue (down). **I**. Bar plots show Normalized Enrichment Score for the top 10 up or down-regulated GSEA-enriched categories. Color, q-value. **J**. GSEA plots for a core subset of gene ontologies are displayed. Data are plotted as the mean ± s.e.m. (**D, E,** and **F**). Statistical significance was evaluated by one-way ANOVA followed by Tukey's post hoc-test (**D**) or Dunnett's post hoc-test (**E**).

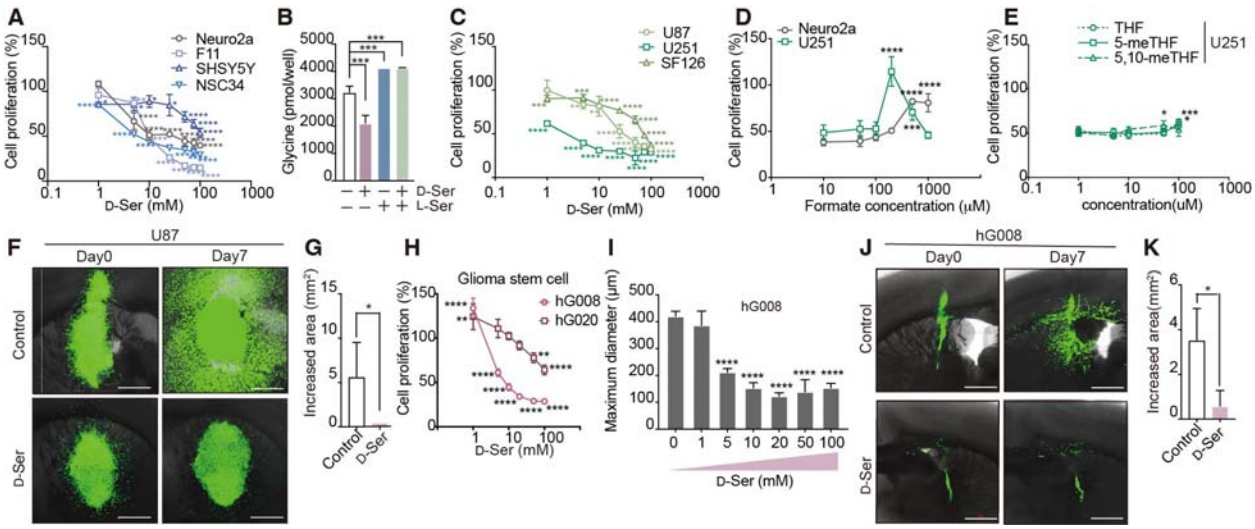

Fig. 3 D-serine attenuates proliferation of neural tumor cells

A, C, H. Relative proliferation of neuroblastoma cell lines (**A**), glioblastoma lines (**C**), and glioma stem cells (**H**) treated with D-serine at indicated doses were analyzed 48 h after treatment (n = 4, each). Cells with the vehicle treatment were used as 100% proliferation controls. **B**. Glycine concentration in Neuro2a cells was quantified 48 h after treatment with D- and/or L-serine (n = 3). **D, E**. Cell proliferation was assessed 48 h after treatment with 5 mM D-serine and formate/folates at indicated doses (n = 4). Cell proliferation was compared to that of cells treated with D-serine alone. **F, G, J, K.** *Ex vivo* slice cultures of mouse brain transplanted with U87 (**F, G**) or hG008 cells (**J, K**) expressing Venus fluorescence were treated with D-serine. Representative images of the xenograft at 0 and 7 days after treatment are shown (**F, J**). Increased area of fluorescence after 7 days of culture was measured (**G, K**). **I**. Sphere diameters of glioma stem cells (hG008) were measured at 7 days after treatment with D-serine at indicated doses. Data are presented as the mean ± s.e.m. (**A-E, G-I,** and **K**). Statistical significance was evaluated by one-way ANOVA followed by Dunnett's post-hoc test (**B, D,** and **E**) or by Student's t-test (**G** and **K**).

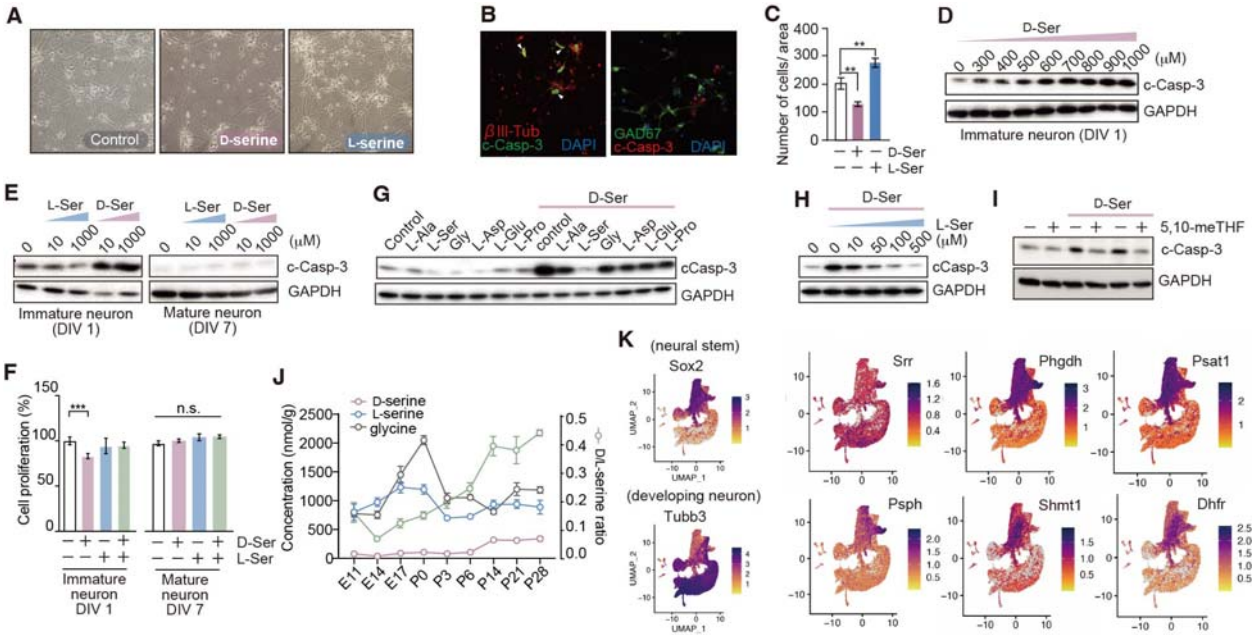

Fig. 4 Developmental transition of serine enantiomer synthesis and enantio-selective effects on immature and mature neurons

A. Light microscopic view showing primary cultured NPCs treated with 1mM D- or L-serine for 7 days in serine-free media. **B.** Immunofluorescent images are NPCs treated with 1 mM D-serine for 48 hours. Cleaved caspase-3 (c-Casp-3), green (left) or red (right); βIII Tubulin, red (left); GAD67, green (right); and DAPI (blue). **C**. Numbers of NPCs per area at DIV7 in (**A**) were counted (n = 4). **D.** Western blots indicate cleavage of caspase-3 in cultured neurons at 48 h after treatment of D-serine with indicated doses. **E.** Western blots indicate cleavage of caspase-3 in cultured neurons at 48 h after treatment of serine enantiomers with indicated doses starting at DIV1 (immature) or DIV7 (mature neurons or astrocytes). **F.** Relative cell proliferation of NPCs after 48 h treatment of 1mM serine enantiomers was analyzed (n = 4). **G. H.** Cleavage of caspase-3 in NPCs induced by 1mM D-serine was observed in the presence of various L-amino acids (1 mM each) (**G**) or L-serine at indicated doses (**H**). **I**. Cleavage of caspase-3 in NPCs triggered by 2 mM D-serine was observed in the presence or absence of 40 μM 5,10-meTHF. **J**. Concentrations of serine enantiomers and glycine and the ratio of serine enantiomer concentrations in the cerebrum during development (n= 3-4). **K**. Single-cell transcriptome profiles of enzymes involved in serine metabolic pathways during mouse brain development. Original data were from Bella et al(Bella et al., 2021). Data are plotted as the mean ± s.e.m. Statistical significance was evaluated by One-way ANOVA followed by Dunnett's post hoc test (**C**). All *in vitro* data are the representative of at least two independent experiments.

679 **References**
680
681

682 Acuna-Hidalgo R, Schanze D, Kariminejad A, Nordgren A, Kariminejad MH, Conner P, Grigelioniene G,
683 Nilsson D, Nordenskjöld M, Wedell A, Freyer C, Wredenberg A, Wieczorek D, Gillessen-Kaesbach G,
684 Kayserili H, Elcioglu N, Ghaderi-Sohi S, Goodarzi P, Setayesh H, van de Vorst M, Steehouwer M,
685 Pfundt R, Krabichler B, Curry C, MacKenzie MG, Boycott KM, Gilissen C, Janecke AR, Hoischen A,
686 Zenker M. 2014. Neu-Laxova Syndrome Is a Heterogeneous Metabolic Disorder Caused by Defects in
687 Enzymes of the L-Serine Biosynthesis Pathway. *Am J Hum Genet* **95**:285–293.
688 doi:10.1016/j.ajhg.2014.07.012

689 Archibald JM. 2015. Endosymbiosis and Eukaryotic Cell Evolution. *Curr Biol* **25**:R911–R921.
690 doi:10.1016/j.cub.2015.07.055

691 Balu DT, Basu AC, Corradi JP, Cacace AM, Coyle JT. 2012. The NMDA receptor co-agonists, d-serine
692 and glycine, regulate neuronal dendritic architecture in the somatosensory cortex. *Neurobiol Dis*
693 **45**:671–682. doi:10.1016/j.nbd.2011.10.006

694 Balu DT, Takagi S, Puhl MD, Benneyworth MA, Coyle JT. 2014. d-Serine and Serine Racemase are
695 Localized to Neurons in the Adult Mouse and Human Forebrain. *Cell Mol Neurobiol* **34**:419–435.
696 doi:10.1007/s10571-014-0027-z

697 Basu AC, Tsai GE, Ma C-L, Ehmsen JT, Mustafa AK, Han L, Jiang ZI, Benneyworth MA, Froimowitz
698 MP, Lange N, Snyder SH, Bergeron R, Coyle JT. 2009. Targeted disruption of serine racemase affects
699 glutamatergic neurotransmission and behavior. *Mol Psychiatry* **14**:719–727. doi:10.1038/mp.2008.130

700 Beaudin AE, Stover PJ. 2009. Insights into metabolic mechanisms underlying folate□responsive neural
701 tube defects: A minireview. *Birth Defects Res Part A: Clin Mol Teratol* **85**:274–284.
702 doi:10.1002/bdra.20553

703 Bella DJD, Habibi E, Stickels RR, Scalia G, Brown J, Yadollahpour P, Yang SM, Abbate C, Biancalani T,
704 Macosko EZ, Chen F, Regev A, Arlotta P. 2021. Molecular logic of cellular diversification in the
705 mouse cerebral cortex. *Nature* **595**:554–559. doi:10.1038/s41586-021-03670-5

706 Bent MJ van den, Geurts M, French PJ, Smits M, Capper D, Bromberg JEC, Chang SM. 2023. Primary
707 brain tumours in adults. *Lancet* **402**:1564–1579. doi:10.1016/s0140-6736(23)01054-1

708 Burke EE, Chenoweth JG, Shin JH, Collado-Torres L, Kim S-K, Micali N, Wang Y, Colantuoni C,
709 Straub RE, Hoeppner DJ, Chen H-Y, Sellers A, Shibbani K, Hamersky GR, Bustamante MD, Phan
710 BN, Ulrich WS, Valencia C, Jaishankar A, Price AJ, Rajpurohit A, Semick SA, Bürli RW, Barrow JC,
711 Hiler DJ, Page SC, Martinowich K, Hyde TM, Kleinman JE, Berman KF, Apud JA, Cross AJ,
712 Brandon NJ, Weinberger DR, Maher BJ, McKay RDG, Jaffe AE. 2020. Dissecting transcriptomic
713 signatures of neuronal differentiation and maturation using iPSCs. *Nat Commun* **11**:462.
714 doi:10.1038/s41467-019-14266-z

715 Chatterton JE, Awobuluyi M, Premkumar LS, Takahashi H, Talantova M, Shin Y, Cui J, Tu S, Sevarino
716 KA, Nakanishi N, Tong G, Lipton SA, Zhang D. 2002. Excitatory glycine receptors containing the
717 NR3 family of NMDA receptor subunits. *Nature* **415**:793–798. doi:10.1038/nature715

718 Cosloy SD, McFall E. 1973. Metabolism of d-Serine in Escherichia coli K-12: Mechanism of Growth
719 Inhibition. *J Bacteriol* **114**:685–694. doi:10.1128/jb.114.2.685-694.1973

720 Delgado-López PD, Corrales-García EM. 2016. Survival in glioblastoma: a review on the impact of
721 treatment modalities. *Clin Transl Oncol* **18**:1062–1071. doi:10.1007/s12094-016-1497-x

722 Ducker GS, Chen L, Morscher RJ, Ghergurovich JM, Esposito M, Teng X, Kang Y, Rabinowitz JD. 2016.
723 Reversal of Cytosolic One-Carbon Flux Compensates for Loss of the Mitochondrial Folate Pathway.
724 *Cell Metab* **23**:1140–1153. doi:10.1016/j.cmet.2016.04.016

725 Ducker GS, Rabinowitz JD. 2017. One-Carbon Metabolism in Health and Disease. *Cell Metab* **25**:27–42.
726 doi:10.1016/j.cmet.2016.08.009

727 Fukaya R, Ohta S, Yaguchi T, Matsuzaki Y, Sugihara E, Okano H, Saya H, Kawakami Y, Kawase T,
728 Yoshida K, Toda M. 2016. MIF Maintains the Tumorigenic Capacity of Brain Tumor–Initiating Cells
729 by Directly Inhibiting p53. *Cancer Res* **76**:2813–2823. doi:10.1158/0008-5472.can-15-1011

730 Furukawa H, Gouaux E. 2003. Mechanisms of activation, inhibition and specificity: crystal structures of
731 the NMDA receptor NR1 ligand-binding core. *The EMBO Journal*. doi:10.1093/emboj/cdg303

732 Fuse S, Sugimoto M, Kurosawa Y, Kuroiwa M, Aita Y, Tomita A, Yamaguchi E, Tanaka R, Endo T,
733 Kime R, Hamaoka T. 2020. Relationships between plasma lipidomic profiles and brown adipose tissue
734 density in humans. *Int J Obes* **44**:1387–1396. doi:10.1038/s41366-020-0558-y

735 Geeraerts SL, Heylen E, Keersmaecker KD, Kampen KR. 2021. The ins and outs of serine and glycine
736 metabolism in cancer. *Nat Metab* **3**:131–141. doi:10.1038/s42255-020-00329-9

737 Gimple RC, Yang K, Halbert ME, Agnihotri S, Rich JN. 2022. Brain cancer stem cells: resilience through
738 adaptive plasticity and hierarchical heterogeneity. *Nat Rev Cancer* **22**:497–514. doi:10.1038/s41568-
739 022-00486-x

740 Gonda Y, Ishii C, Mita M, Nishizaki N, Ohtomo Y, Hamase K, Shimizu T, Sasabe J. 2022. Astrocytic
741 d□amino acid oxidase degrades d□serine in the hindbrain. *FEBS Lett* **596**:2889–2897.
742 doi:10.1002/1873-3468.14417

743 Gonda Y, Matsuda A, Adachi K, Ishii C, Suzuki M, Osaki A, Mita M, Nishizaki N, Ohtomo Y, Shimizu
744 T, Yasui M, Hamase K, Sasabe J. 2023. Mammals sustain amino acid homochirality against chiral
745 conversion by symbiotic microbes. *Proc Natl Acad Sci U S A*. doi:10.1073/pnas.2300817120

746 Hashimoto A, Nishikawa T, Oka T, Takahashi K. 1993. Endogenous d□Serine in Rat Brain:
747 N□Methyl□d□Aspartate Receptor□Related Distribution and Aging. *J Neurochem* **60**:783–786.
748 doi:10.1111/j.1471-4159.1993.tb03219.x

749 Hirabayashi Y, Furuya S. 2008. Roles of l-serine and sphingolipid synthesis in brain development and
750 neuronal survival. *Prog Lipid Res* **47**:188–203. doi:10.1016/j.plipres.2008.01.003

751 Horn MRV, Strasser A, Miraucourt LS, Pollegioni L, Ruthazer ES. 2017. The Gliotransmitter d-Serine
752 Promotes Synapse Maturation and Axonal Stabilization In Vivo. *J Neurosci* **37**:6277–6288.
753 doi:10.1523/jneurosci.3158-16.2017

754 Hubbard KS, Gut IM, Lyman ME, McNutt PM. 2013. Longitudinal RNA sequencing of the deep
755 transcriptome during neurogenesis of cortical glutamatergic neurons from murine ESCs.
756 *F1000research* **2**:35. doi:10.12688/f1000research.2-35.v1

757 Inoue R, Hashimoto K, Harai T, Mori H. 2008. NMDA- and β-Amyloid1–42-Induced Neurotoxicity Is
758 Attenuated in Serine Racemase Knock-Out Mice. *J Neurosci* **28**:14486–14491.
759 doi:10.1523/jneurosci.5034-08.2008

760 Ishii C, Akita T, Mita M, Ide T, Hamase K. 2018. Development of an online two-dimensional high-
761 performance liquid chromatographic system in combination with tandem mass spectrometric detection
762 for enantiomeric analysis of free amino acids in human physiological fluid. *J Chromatogr A* **1570**:91–
763 98. doi:10.1016/j.chroma.2018.07.076

764 Jaeken J, Detheux M, Fryns JP, Collet JF, Alliet P, Schaftingen EV. 1997. Phosphoserine phosphatase
765 deficiency in a patient with Williams syndrome. *J Méd Genet* **34**:594. doi:10.1136/jmg.34.7.594

766 Jain M, Nilsson R, Sharma S, Madhusudhan N, Kitami T, Souza AL, Kafri R, Kirschner MW, Clish CB,
767 Mootha VK. 2012. Metabolite profiling identifies a key role for glycine in rapid cancer cell
768 proliferation. *Science* **336**:1037–1040. doi:10.1126/science.1218595

769 Kaltenbach JP, Ganote CE, Carone FA. 1979. Renal tubular necrosis induced by compounds structurally
770 related to d-serine. *Exp Mol Pathol* **30**:209–214. doi:10.1016/0014-4800(79)90054-6

771 Klepinin A, Ounpuu L, Guzun R, Chekulayev V, Timohhina N, Tepp K, Shevchuk I, Schlattner U,
772 Kaambre T. 2016. Simple oxygraphic analysis for the presence of adenylate kinase 1 and 2 in normal
773 and tumor cells. *J Bioenerg Biomembr* **48**:531–548. doi:10.1007/s10863-016-9687-3

774 KONING TJD, DURAN M, MALDERGEM LV, PINEDA M, DORLAND1 L, GOOSKENS R, POLL-T
775 JJ and BT. 2002. Congenital microcephaly and seizures due to 3-phosphoglycerate dehydrogenase
776 deficiency: Outcome of treatment with amino acids. *J Inherit Metab Dis*.

777 Kory N, Wyant GA, Prakash G, Bos J uit de, Bottanelli F, Pacold ME, Chan SH, Lewis CA, Wang T,
778 Keys HR, Guo YE, Sabatini DM. 2018. SFXN1 is a mitochondrial serine transporter required for one-
779 carbon metabolism. *Science* **362**. doi:10.1126/science.aat9528

780 Kuznetsov AV, Veksler V, Gellerich FN, Saks V, Margreiter R, Kunz WS. 2008. Analysis of
781 mitochondrial function in situ in permeabilized muscle fibers, tissues and cells. *Nat Protoc* **3**:965–976.
782 doi:10.1038/nprot.2008.61

783 Labuschagne CF, van den Broek NJF, Mackay GM, Vousden KH, Maddocks ODK. 2014. Serine, but Not
784 Glycine, Supports One-Carbon Metabolism and Proliferation of Cancer Cells. *Cell Reports* **7**:1248–
785 1258. doi:10.1016/j.celrep.2014.04.045

786 Lee GY, Haverty PM, Li L, Kljavin NM, Bourgon R, Lee J, Stern H, Modrusan Z, Seshagiri S, Zhang Z,
787 Davis D, Stokoe D, Settleman J, Sauvage FJ de, Neve RM. 2014. Comparative Oncogenomics
788 Identifies PSMB4 and SHMT2 as Potential Cancer Driver Genes. *Cancer Res* **74**:3114–3126.
789 doi:10.1158/0008-5472.can-13-2683

Lee Y, Wiriyasermkul P, Kongpracha P, Moriyama S, Mills DJ, Kühlbrandt W, Nagamori S. 2022. Ca2+-mediated higher-order assembly of heterodimers in amino acid transport system b0,+ biogenesis and cystinuria. *Nat Commun* **13**:2708. doi:10.1038/s41467-022-30293-9

Lewis CA, Parker SJ, Fiske BP, McCloskey D, Gui DY, Green CR, Vokes NI, Feist AM, Vander Heiden MG, Metallo CM. 2014. Tracing Compartmentalized NADPH Metabolism in the Cytosol and Mitochondria of Mammalian Cells. *Mol Cell* **55**:253–263. doi:10.1016/j.molcel.2014.05.008

Lynch JW. 2004. Molecular Structure and Function of the Glycine Receptor Chloride Channel. *Physiol Rev* **84**:1051–1095. doi:10.1152/physrev.00042.2003

MacFarlane AJ, Liu X, Perry CA, Flodby P, Allen RH, Stabler SP, Stover PJ. 2008. Cytoplasmic Serine Hydroxymethyltransferase Regulates the Metabolic Partitioning of Methylenetetrahydrofolate but Is Not Essential in Mice*. *J Biol Chem* **283**:25846–25853. doi:10.1074/jbc.m802671200

Maekawa M, Okamura T, Kasai N, Hori Y, Summer KH, Konno R. 2005. d-Amino-acid Oxidase Is Involved in d-Serine-Induced Nephrotoxicity. *Chem Res Toxicol* **18**:1678–1682. doi:10.1021/tx0500326

McNamara D, Dingledine R. 1990. Dual effect of glycine on NMDA-induced neurotoxicity in rat cortical cultures. *J Neurosci* **10**:3970–3976. doi:10.1523/jneurosci.10-12-03970.1990

Miya K, Inoue R, Takata Y, Abe M, Natsume R, Sakimura K, Hongou K, Miyawaki T, Mori H. 2008. Serine racemase is predominantly localized in neurons in mouse brain. *J Comp Neurol* **510**:641–654. doi:10.1002/cne.21822

Miyamoto T, Fushinobu S, Saitoh Y, Sekine M, Katane M, Sakai□Kato K, Homma H. 2024. Novel tetrahydrofolate□dependent d□serine dehydratase activity of serine hydroxymethyltransferases. *FEBS J* **291**:308–322. doi:10.1111/febs.16953

Miyoshi Y, Hamase K, Tojo Y, Mita M, Konno R, Zaitsu K. 2009. Determination of d-serine and d-alanine in the tissues and physiological fluids of mice with various d-amino-acid oxidase activities using two-dimensional high-performance liquid chromatography with fluorescence detection. *J Chromatogr B* **877**:2506–2512. doi:10.1016/j.jchromb.2009.06.028

Mothet J-P, Parent AT, Wolosker H, Brady RO, Linden DJ, Ferris CD, Rogawski MA, Snyder SH. 2000. d-Serine is an endogenous ligand for the glycine site of the N-methyl-d-aspartate receptor. *Proc Natl Acad Sci* **97**:4926–4931. doi:10.1073/pnas.97.9.4926

Mustafa AK, Ahmad AS, Zeynalov E, Gazi SK, Sikka G, Ehmsen JT, Barrow RK, Coyle JT, Snyder SH, Doré S. 2010. Serine Racemase Deletion Protects Against Cerebral Ischemia and Excitotoxicity. *J Neurosci* **30**:1413–1416. doi:10.1523/jneurosci.4297-09.2010

Nagata Y, Horiike K, Maeda T. 1994. Distribution of freed-serine in vertebrate brains. *Brain Res* **634**:291–295. doi:10.1016/0006-8993(94)91932-1

Nancy KW, Dingledine R. 1988. Requirement for Glycine in Activation of NMDA-Receptors Expressed in Xenopus Oocytes. *science*.

826 Newman AC, Maddocks ODK. 2017. One-carbon metabolism in cancer. *Br J Cancer* **116**:1499–1504.
827 doi:10.1038/bjc.2017.118

828 Nilsson R, Jain M, Madhusudhan N, Sheppard NG, Strittmatter L, Kampf C, Huang J, Asplund A,
829 Mootha VK. 2014. Metabolic enzyme expression highlights a key role for MTHFD2 and the
830 mitochondrial folate pathway in cancer. *Nat Commun* **5**:3128. doi:10.1038/ncomms4128

831 Nomura J, Jaaro-Peled H, Lewis E, Nuñez-Abades P, Huppe-Gourgues F, Cash-Padgett T, Emiliani F,
832 Kondo MA, Furuya A, Landek-Salgado MA, Ayhan Y, Kamiya A, Takumi T, Huganir R, Pletnikov
833 M, O'Donnell P, Sawa A. 2016. Role for neonatal D-serine signaling: prevention of physiological and
834 behavioral deficits in adult Pick1 knockout mice. *Mol Psychiatry* **21**:386–393.
835 doi:10.1038/mp.2015.61

836 Okada A, Nangaku M, Jao T-M, Maekawa H, Ishimono Y, Kawakami T, Inagi R. 2017. D-serine, a novel
837 uremic toxin, induces senescence in human renal tubular cells via GCN2 activation. *Sci Rep* **7**:11168.
838 doi:10.1038/s41598-017-11049-8

839 Pan S, Fan M, Liu Z, Li X, Wang H. 2020. Serine, glycine and one-carbon metabolism in cancer
840 (Review). *Int J Oncol* **58**:158–170. doi:10.3892/ijo.2020.5158

841 Pang Z, Chong J, Zhou G, de Lima Morais DA, Chang L, Barrette M, Gauthier C, Jacques P-É, Li S, Xia
842 J. 2021. MetaboAnalyst 5.0: narrowing the gap between raw spectra and functional insights. *Nucleic*
843 *Acids Res* **49**:gkab382-. doi:10.1093/nar/gkab382

844 Patel J, Zinkand WC, Thompson C, Keith R, Salama A. 1990. Role of Glycine in the
845 N□Methyl□d□Aspartate□Mediated Neuronal Cytotoxicity. *J Neurochem* **54**:849–854.
846 doi:10.1111/j.1471-4159.1990.tb02329.x

847 Reya T, Morrison SJ, Clarke MF, Weissman IL. 2001. Stem cells, cancer, and cancer stem cells. *Nature*
848 **414**:105–111. doi:10.1038/35102167

849 Sasabe J, Chiba T, Yamada M, Okamoto K, Nishimoto I, Matsuoka M, Aiso S. 2007. D□Serine is a key
850 determinant of glutamate toxicity in amyotrophic lateral sclerosis. *EMBO J* **26**:4149–4159.
851 doi:10.1038/sj.emboj.7601840

852 Shleper M, Kartvelishvily E, Wolosker H. 2005. D-Serine Is the Dominant Endogenous Coagonist for
853 NMDA Receptor Neurotoxicity in Organotypic Hippocampal Slices. *J Neurosci* **25**:9413–9417.
854 doi:10.1523/jneurosci.3190-05.2005

855 Sultan S, Li L, Moss J, Petrelli F, Cassé F, Gebara E, Lopatar J, Pfrieger FW, Bezzi P, Bischofberger J,
856 Toni N. 2015. Synaptic Integration of Adult-Born Hippocampal Neurons Is Locally Controlled by
857 Astrocytes. *Neuron* **88**:957–972. doi:10.1016/j.neuron.2015.10.037

858 Tajan M, Hennequart M, Cheung EC, Zani F, Hock AK, Legrave N, Maddocks ODK, Ridgway RA,
859 Athineos D, Suárez-Bonnet A, Ludwig RL, Novellasdemunt L, Angelis N, Li VSW, Vlachogiannis G,
860 Valeri N, Mainolfi N, Suri V, Friedman A, Manfredi M, Blyth K, Sansom OJ, Vousden KH. 2021.
861 Serine synthesis pathway inhibition cooperates with dietary serine and glycine limitation for cancer
862 therapy. *Nat Commun* **12**:366. doi:10.1038/s41467-020-20223-y

Tamura R, Miyoshi H, Sampetrean O, Shinozaki M, Morimoto Y, Iwasawa C, Fukaya R, Mine Y, Masuda H, Maruyama T, Narita M, Saya H, Yoshida K, Okano H, Toda M. 2019. Visualization of spatiotemporal dynamics of human glioma stem cell invasion. *Mol Brain* **12**:45. doi:10.1186/s13041-019-0462-3

Tang X, Zuo C, Fang P, Liu G, Qiu Y, Huang Y, Tang R. 2021. Targeting Glioblastoma Stem Cells: A Review on Biomarkers, Signal Pathways and Targeted Therapy. *Front Oncol* **11**:701291. doi:10.3389/fonc.2021.701291

Tomita A, Mori M, Hiwatari K, Yamaguchi E, Itoi T, Sunamura M, Soga T, Tomita M, Sugimoto M. 2018. Effect of storage conditions on salivary polyamines quantified via liquid chromatography-mass spectrometry. *Sci Rep* **8**:12075. doi:10.1038/s41598-018-30482-x

Williams RE, Lock EA. 2004. d-Serine-induced nephrotoxicity: possible interaction with tyrosine metabolism. *Toxicology* **201**:231–238. doi:10.1016/j.tox.2004.05.001

Wiriyasermkul P, Nagamori S, Tominaga H, Oriuchi N, Kaira K, Nakao H, Kitashoji T, Ohgaki R, Tanaka H, Endou H, Endo K, Sakurai H, Kanai Y. 2012. Transport of 3-Fluoro-l-α-Methyl-Tyrosine by Tumor-Upregulated L-Type Amino Acid Transporter 1: A Cause of the Tumor Uptake in PET. *J Nucl Med* **53**:1253–1261. doi:10.2967/jnumed.112.103069

Wolosker H. 2011. Serine racemase and the serine shuttle between neurons and astrocytes. *Biochimica Et Biophysica Acta Bba - Proteins Proteom* **1814**:1558–1566. doi:10.1016/j.bbapap.2011.01.001

Wolosker H, Balu DT. 2020. d-Serine as the gatekeeper of NMDA receptor activity: implications for the pharmacologic management of anxiety disorders. *Transl Psychiatry* **10**:184. doi:10.1038/s41398-020-00870-x

Yang JH, Wada A, Yoshida K, Miyoshi Y, Sayano T, Esaki K, Kinoshita MO, Tomonaga S, Azuma N, Watanabe M, Hamase K, Zaitsu K, Machida T, Messing A, Itohara S, Hirabayashi Y, Furuya S. 2010. Brain-specific Phgdh Deletion Reveals a Pivotal Role for l-Serine Biosynthesis in Controlling the Level of d-Serine, an N-methyl-d-aspartate Receptor Co-agonist, in Adult Brain*. *J Biol Chem* **285**:41380–41390. doi:10.1074/jbc.m110.187443

Yoshida K, Furuya S, Osuka S, Mitoma J, Shinoda Y, Watanabe M, Azuma N, Tanaka H, Hashikawa T, Itohara S, Hirabayashi Y. 2004. Targeted Disruption of the Mouse 3-Phosphoglycerate Dehydrogenase Gene Causes Severe Neurodevelopmental Defects and Results in Embryonic Lethality*. *J Biol Chem* **279**:3573–3577. doi:10.1074/jbc.c300507200